

# PROCEEDINGS OF SPIE

[SPIDigitalLibrary.org/conference-proceedings-of-spie](https://spiedigitallibrary.org/conference-proceedings-of-spie)

## Simulation of damage-features in complex joint using guided waves

Sunilkumar Soni, Sourav Banerjee, Santanu Das, Aditi Chattopadhyay

Sunilkumar Soni, Sourav Banerjee, Santanu Das, Aditi Chattopadhyay, "Simulation of damage-features in complex joint using guided waves," Proc. SPIE 6926, Modeling, Signal Processing, and Control for Smart Structures 2008, 69260O (3 April 2008); doi: 10.1117/12.776468

**SPIE.**

Event: SPIE Smart Structures and Materials + Nondestructive Evaluation and Health Monitoring, 2008, San Diego, California, United States

# Simulation of Damage-Features in Complex Joint using Guided Waves

Sunilkumar Soni\*<sup>a</sup>, Sourav Banerjee<sup>b</sup>, Santanu Das<sup>c</sup>, Aditi Chattopadhyay<sup>a,b</sup>

<sup>a</sup>Department of Mechanical and Aerospace Engineering, Arizona State University, Tempe, Arizona, USA 85287-6106

<sup>b</sup>Adaptive Intelligent Materials & Systems (AIMS) Center, Arizona State University, Tempe, Arizona, USA 85287-6106

<sup>c</sup>NASA Ames Research Center, Building 269, Moffett Field, CA, USA 94035

## ABSTRACT

This paper presents the use of guided wave concept in localizing small cracks in complex lug joint structures. A lug joint is one of the several ‘hotspots’ in an aerospace structure which experiences fatigue damage. Several fatigue tests on lug joint samples prepared from 0.25” plate of Aluminum (Al) 2024 T351 indicated a distinct failure pattern. All samples failed at the shoulders. Different notch sizes are introduced at the shoulders and both virtual and real active health monitoring with piezoelectric transducers is performed. Simulations of the real time experiment are carried out using Finite Element (FE) analysis. Similar crack geometry and piezoelectric transducer orientation are considered both in experiment and in simulation. Results presented illustrate the use of guided waves in interrogating damage in lug joints. A comparison of sensor signals has been made between experimental and simulated signals which show good correlation. The frequency transform on the sensor signal data yield useful information for characterizing damage. Further, sensitivity studies are performed. The sensitivity study information offers potential application in reducing the computational cost for any defect localization technique by reducing redundant sensors. This information is a key to optimal sensor placement for damage detection in structural health monitoring (SHM).

**Keywords:** Guided wave, complex geometry, damage interrogation, finite element analysis, fatigue cracks, sensor sensitivity, data pruning technique, piezoelectric, structural health monitoring

## 1. INTRODUCTION

Ultrasonic or acoustic waves are used for nondestructive testing in aircraft industries. A number of techniques have been investigated by researchers to generate ultrasonic waves in solid structures. However, conventional ultrasonic techniques involve localized scanning of a damaged region in a structure for classification and detection. But these techniques are very labor intensive, time consuming and above all not efficient in interrogating large areas of a structure. Hence, the guided wave inspection technique was introduced in the SHM arena by several researchers over the past decade. Guided waves are formed in surface bounded structures due to multiple reflections and refractions from the plate boundaries. They occur in symmetric and antisymmetric modes which cause stretching and bending of the structure respectively. Different modes are sensitive to different type of defects which enables in efficient damage detection. These waves have thus demonstrated their potential in monitoring large areas of metallic aircraft fuselage [1]. However, their dispersive nature and existence of multiple modes make them complicated to use. A detailed description on guided waves can be found in [2-3]. The need for onboard structural health monitoring has led to an increased interest in using piezoelectric sensors/actuators, which are cheaper and light weight compared to the conventional transducers. Piezoelectric wafers can act both as actuators and sensors due to their intrinsic electromechanical coupling. Analytical behavior of two dimensional patches of piezoelectric materials bonded on the surface of distributed systems was studied in [4]. It was proposed that by tailoring the shape of the actuator to either excite or suppress certain modes lead to improved control behavior. Piezoelectric actuators were explored for different excitation signals (continuous sinusoidal and pulse) to study the influence of flaws on Lamb waves for damage detection [5-8]. Several other researchers have made use of piezoelectric sensors for damage detection in beams and large plates using pitch-catch, pulse echo and phased array methods [9-11].

\*Sunilkumar.soni@asu.edu; phone 1 480 965 2434; fax 1 480 965 1384

In structures with complex geometry, separation of symmetric and antisymmetric modes becomes difficult. This increases the complexity in studying the influence of damages on the overlapping modes. In the current paper, a study is conducted on lug joints which represent a typical structural hotspot. Finite element analysis is conducted with piezoelectric wafer bonded to the host structure. Piezoelectrical-mechanical coupling is considered to simulate sensor signals. The signals obtained are further analyzed to study the sensor sensitivities with different levels of damage. A classification technique based on data pruning method [12] is adopted to classify sensor data for different damage states.

## 2. EXPERIMENTAL SETUP

The lug samples were made from 0.25” thick Al 2024-T351 alloy plate. The dimensions of the sample are as shown in Fig. 1. They had sand blasted surface finish. It was observed from the fatigue tests conducted on these samples that they fail at the shoulders [13] (see Fig. 2). Based on those observations, Electrical Discharge Machining notches of length 2mm and 4mm were made in the lug samples. Sensor signals were acquired on the damaged sample and the healthy sample which was used as reference.

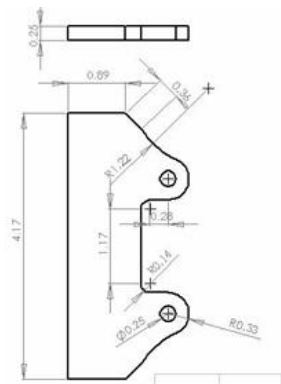


Fig. 1. Dimensions of the Lug Sample



Fig. 2. Failure under fatigue loading

Three piezoelectric sensors and one actuator (APC 850) were glued to the surface around the notches while two more sensors were placed along the thickness direction. The sensor-actuator configuration is as shown in Fig. 3. This placement of the sensors was intuitive and the sensitivity study presented in this paper is expected to help formulate an optimal sensor configuration for localizing and characterizing damage. A 4.5 cycles, 130 KHz tone burst (see Fig. 4) was used as the actuation signal. Sensor signals were collected for all the sensors at a sampling rate of 2 MHz.

## 3. MODELING

A three dimensional Finite Element (FE) modeling is done for the lug sample in the commercial FE software ABAQUS/Standard [14]. The material properties of the lug, adhesive layer and the piezoelectric transducer are listed in Table 1.

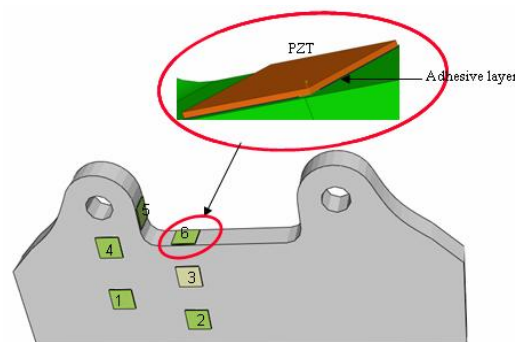


Fig. 3. Lug Geometry

The lug is modeled as an isotropic, homogeneous material. It is made of alumina 2024-T351 and continuum three dimensional brick elements (C3D8R) are used to mesh it. The mesh size varies for samples with different levels of crack (notch) lengths. The adhesive layer is also modeled as an isotropic, homogenous material and continuum three dimensional brick elements (C3D8R) are used for meshing the structure. The piezoelectric transducer is modeled as an orthotropic material with properties defined in the local orientation system. Continuum three dimensional piezoelectric elements (C3D8E) are used to model it. All the degrees of freedom are suppressed at a corner node of the lug as shown in Fig. 5. Tone burst excitation of hundred volts peak to peak is applied to the upper surface of the actuator while the bottom surface is maintained at zero volt.

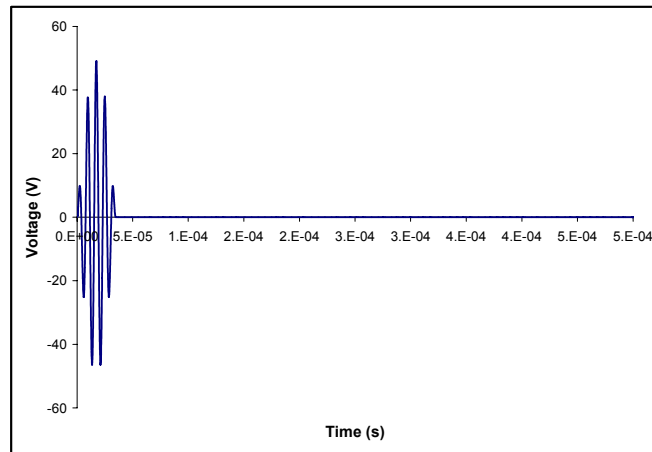


Fig. 4. Actuator Signal

Table 1. Material properties of alumina, adhesive layer and piezoelectric sensors and actuators

Material properties		
	Young's Modulus (Pa)	Density (kg/m <sup>3</sup> )
Aluminum	7.00E+10	2780
Layer	2.75E+09	1050

Piezoelectric sensors (PZT APC 850)					
Elastic Properties					
Elastic Moduli (Pa)		Poisson's ratios		Shear Moduli (Pa)	
E1	6.30E+10	n12	0.301	G12	2.35E+10
E2	6.30E+10	n13	0.532	G13	2.30E+10
E3	5.40E+10	n23	0.532	G23	2.30E+10
Density (Kg/m <sup>3</sup> )	7.50E+03				
Piezoelectric Properties (m/Volt)					
d1 11	0	d2 11	0	d3 11	-1.75E-10
d1 22	0	d2 22	0	d3 22	-1.75E-10
d1 33	0	d2 33	0	d3 33	4.00E-10
d1 12	0	d2 12	0	d3 12	0
d1 13	5.90E-10	d2 13	0	d3 13	0
d1 23	0	d2 23	5.90E-10	d3 23	0
Dielectric (Farad/m)					
D11	1.51E-08	D22	1.51E-08	D33	1.30E-08

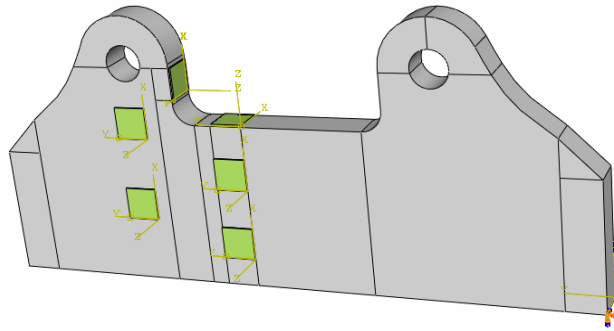


Fig. 5. Boundary Condition

## 4. RESULTS AND DISCUSSIONS

### 4.1 Sensor Signals Obtained From Experiments and Models

Figure 6 shows snapshots of guided waves originating from the actuator and propagating through the lug sample. The snapshots are presented for the healthy sample and the sample with 4mm crack. It can be seen that as the guided waves propagate in the damaged structure, they interact with the crack and a part of the wave energy is reflected back.

The time history of sensor 1 signal calculated experimentally and through simulation, for the healthy case, is presented in Fig. 7. Figure 8 shows the frequency transform obtained using data from sensor 1, 2 and 4. The frequency contents and the corresponding amplitudes are presented in Tables 2 – 4. A fairly good correlation is observed and the differences can be attributed to the simplifications made in modeling (such as perfect bonding between the piezoelectric transducer and host structure, temperature effects, experimental noise etc.).

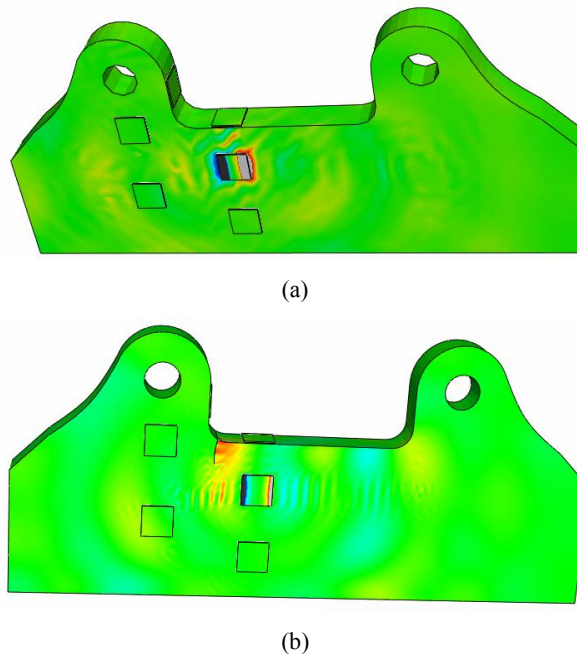


Fig. 6. Guided Wave Propagation in (a) Healthy Lug Sample and (b) 4mm Cracked Sample

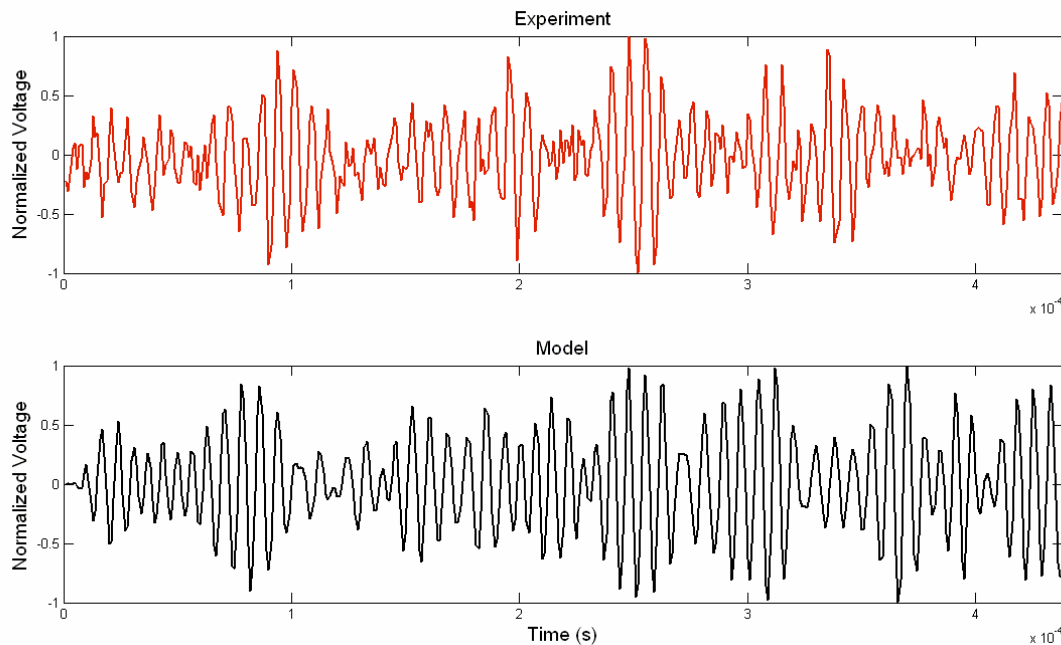


Fig. 7. Time histories of sensor 1 for healthy lug sample

As seen from Table 2, for sensor 1, the amplitude of the frequency spectrum at 125 KHz remains almost unaffected. However, the amplitudes at 138 KHz and 145 KHz are attenuated significantly followed by a mode conversion. For example, the amplitude of 220 associated with 138 KHz frequency in the healthy state translates to 135 KHz and 140 KHz frequency with amplitudes of 125 and 140 respectively for a 2mm crack. A similar transformation is seen for the amplitude associated with 145 KHz frequency for a 4mm crack. From Table 3, for sensor 2, it can be observed that the amplitude associated with 138 KHz frequency translates to 133 KHz and 140 KHz frequency with higher amplitudes both in case of 2mm crack and 4mm crack. Also, the amplitudes increased with increased levels of damage. It must be noted that larger the crack, stronger will be the energy which is reflected back from the crack. Similarly it can be seen from Table 4, for sensor 4, the amplitude of 200 associated with 118 KHz frequency translates to 118 KHz and 122 KHz frequency with amplitudes of 85 and 325 respectively. The amplitudes at these frequencies decreased with increased level of damage. This trend is observed for sensor 4 as it is placed on the other side of the crack (see Fig. 6). Therefore, in this case smaller the crack, faster will be the energy reaching this sensor

The frequency analysis does show that a band of frequencies are excited between the ranges of 100 KHz to 160 KHz. Therefore the product of frequency and thickness ('fd') for this sample lies between 0.625 MHz-mm to 1 MHz-mm. From the dispersion curve for aluminum (see Fig. 9), it can be seen that only the first symmetric ( $S_0$ ) and antisymmetric ( $A_0$ ) modes are generated for this range of 'fd'. The phase velocities corresponding to the  $S_0$  mode remains more or less at 5200 m/s and for  $A_0$  mode lie in the range of 2000 – 2400 m/s. The group velocities range between 5000 – 5250 m/s for  $S_0$  mode and remains more or less at 3100 m/s for  $A_0$  mode. Based on the group velocity information, the presence of the  $A_0$  mode has been clearly observed at the receiver end. This is true as the actuator was mounted only on one side of the sample surface and caused actuation of antisymmetric modes. It cannot be concluded that the  $S_0$  mode was not generated but the energy associated with it is very small. Also,  $S_0$  modes experience higher attenuation as compared to  $A_0$  modes while propagating in the media.

The frequency analysis for given sensors (with given locations) contains information that can be used to characterize the nature of the crack e.g. magnitude and orientation. Therefore, it is observed that changes (localized) in the dynamics of the system have influenced the magnitude and phase of the frequency contents of each sensor, with a given location. Hence this study is useful for defect characterization once the sensor location is determined.

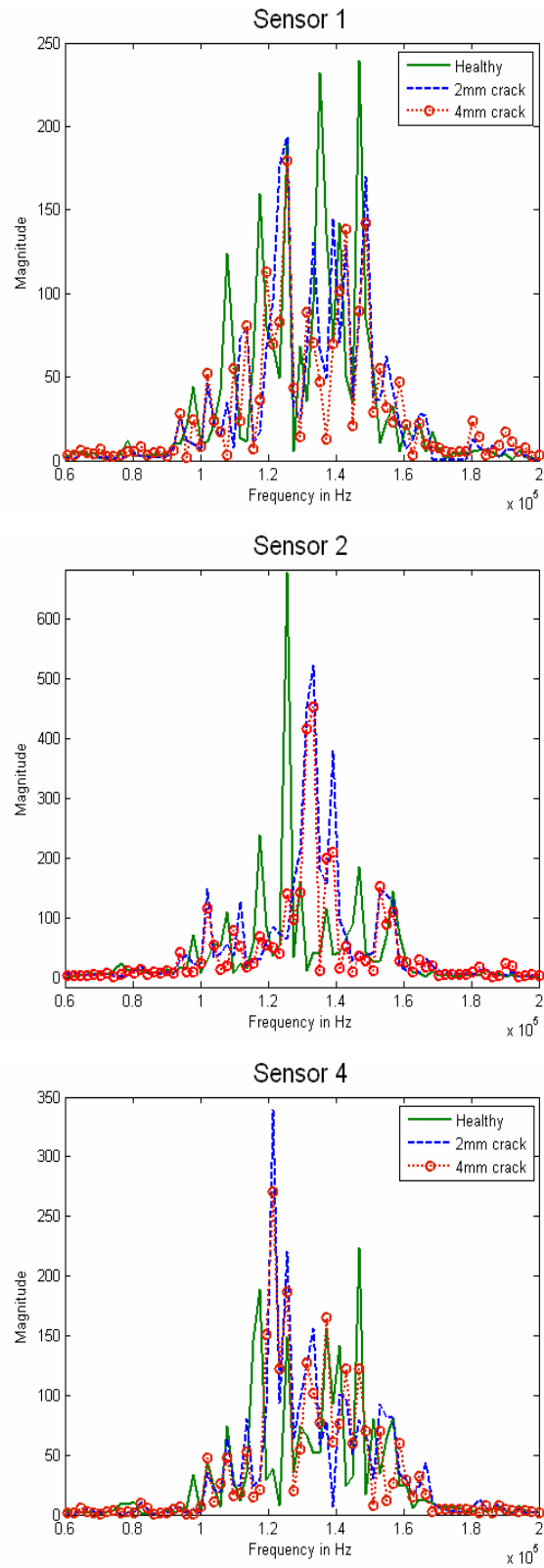


Fig. 8. Frequency comparison of sensor 1, sensor 2 and sensor 4 for different states of the lug joint

Table 2. Frequency information comparison for sensor 1

Sensor 1					
Healthy		2mm		4mm	
Frequency (KHz)	Amplitude	Frequency (KHz)	Amplitude	Frequency (KHz)	Amplitude
98	30	-	-		
108	120	108	115		
				113	80
118	180	118	85		
				120	100
125	200	125	200	125	150
130	-				
		<b>135</b>	125	<b>133</b>	85
<b>138</b>	220				
		<b>140</b>	140	<b>142</b>	138
<b>145</b>	250				
		<b>150</b>	160	<b>150</b>	150
158	-				

Table 3. Frequency information comparison for sensor 2

Sensor 2					
Healthy		2mm		4mm	
Frequency (KHz)	Amplitude	Frequency (KHz)	Amplitude	Frequency (KHz)	Amplitude
98	90	-	-		
		101	110	101	170
108	110	108	85		
118	250	118	50	118	135
125	680	125	150	-	-
130	150				
		<b>133</b>	450	<b>133</b>	550
<b>138</b>	130				
		<b>140</b>	200	<b>140</b>	395
145	-				
158	150	158	150	158	150

Table 4. Frequency information comparison for sensor 4

Sensor 4					
Healthy		2mm		4mm	
Frequency (KHz)	Amplitude	Frequency (KHz)	Amplitude	Frequency (KHz)	Amplitude
98	45	-	-	-	-
108	80	101	35	101	35
		108	75	108	35
<b>118</b>	200	<b>118</b>	85	<b>118</b>	40
		<b>122</b>	325	<b>122</b>	290
<b>125</b>	150	<b>125</b>	220	<b>125</b>	180
130	-				
				133	120
138	150	138	75	138	150
145	220	145	110	145	130
158	-	158	-	158	-

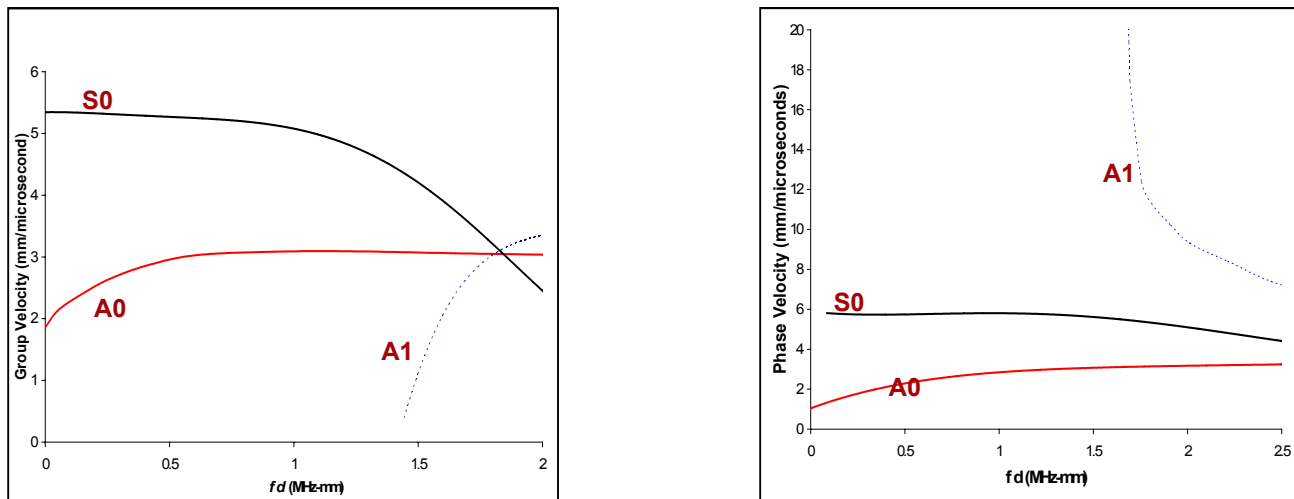


Fig. 9. Dispersion curve for traction free Aluminum plate

#### 4.2 Determination of sensor sensitivities

It is essential from optimal sensor placement point of view to measure sensor sensitivities for the current structure and sensor architecture. In general a damaged sensor signal state has significant deviation from the healthy state signals. This anomaly detection in the sensor signals can be associated with the pattern recognition problem that looks for anomalous changes in the sensor signal also termed as outlier detection. The outliers can be defined by their distance to neighboring examples. The detection of outliers has a long history in statistics [15, 16], however the methods discussed are largely for univariate data and with a parametric distribution. Many researchers have therefore proposed methods to overcome the limitation of known distribution using nearest neighbor based approaches [17-19]. The biggest problem, however, is the quadratic scaling behavior which increases the computational time with increase in the size of the data set.

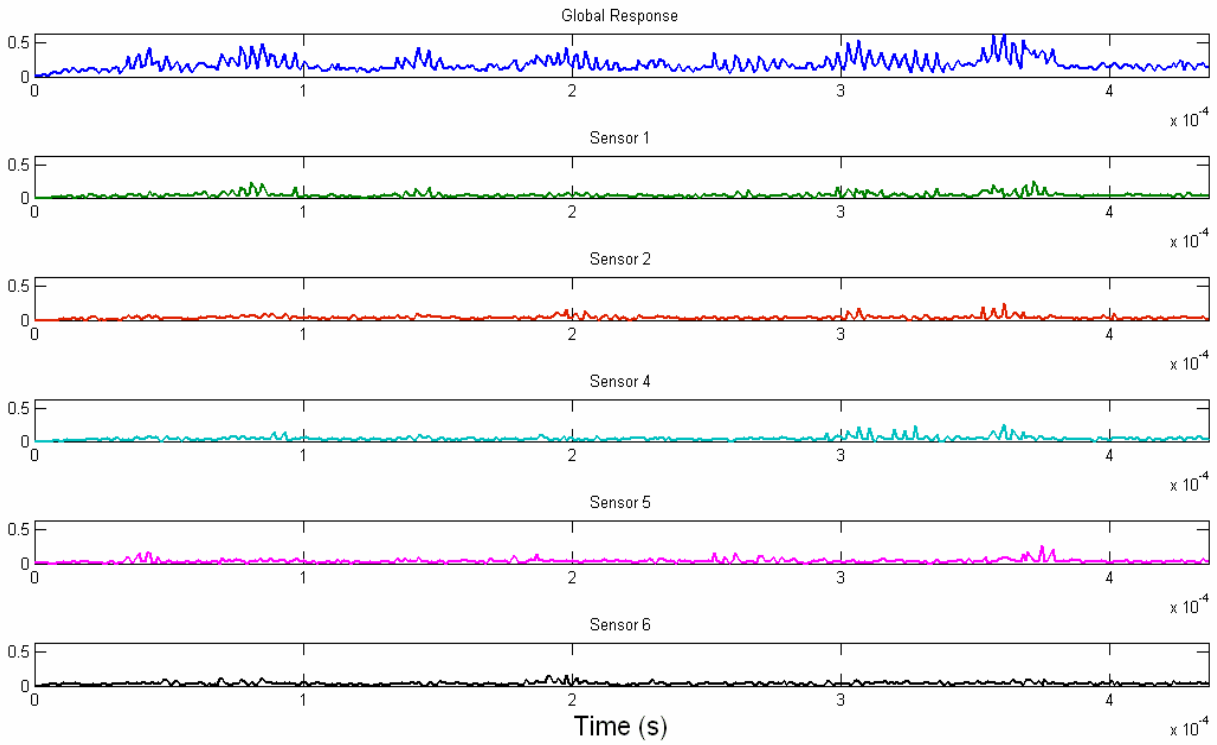


Fig. 10. Global response of the sensors and the individual sensor sensitivity for 2mm crack

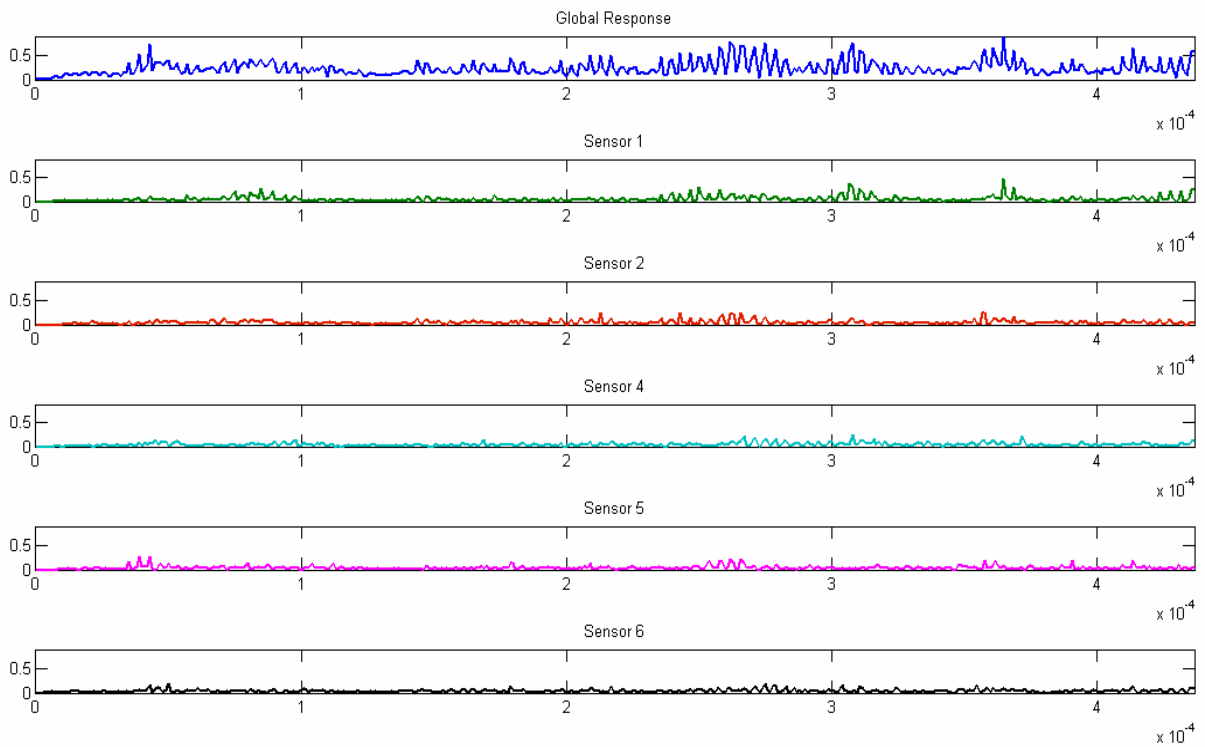


Fig. 11. Global response of the sensors and the individual sensor sensitivity for 4mm crack

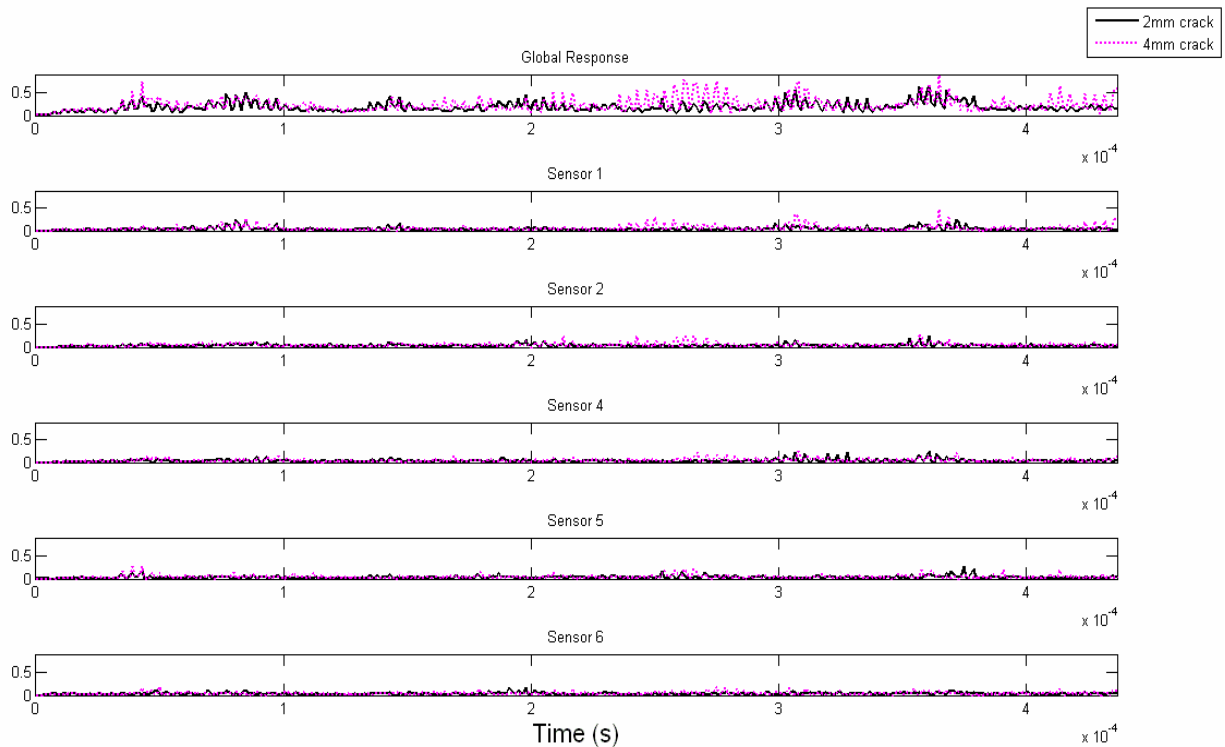


Fig. 12. Comparison of sensor sensitivities for 2mm and 4mm crack

A modified nested loop method can be used to solve high dimensional data sets [12]. The authors proposed a  $k$ -nearest neighbor based algorithm (called ‘ORCA\*’) based on nested loops in conjunction with randomization and simple pruning rule such that near linear performance can be obtained while analyzing large data sets. In the present study ORCA was extended to calculate the sensor sensitivity in the presence of damages with different length scales. The algorithm uses a distance-based metric for finding outlier by examining the distance of any test point to  $k$  existing examples those considered as nearest neighbors. If one looks at the local neighborhood and finds that the test points are relatively close, then the examples are considered normal or else unusual. The advantages of distance-based outliers are that no explicit distribution needs to be defined to determine unusualness, and that it can be applied to any feature space for which we can define a distance measure. Further details of this algorithm can be obtained in [12].

Table 5. Individual sensor sensitivity contribution to the global response for 2mm and 4mm crack lengths

Sensor Sensitivity ( in Percentage)		
Sensor ID	2mm crack	4mm crack
S1	22.298	23.896
S2	19.905	20.468
S4	20.164	19.326
S5	18.8	18.203
S6	18.833	17.941

The first plot in Fig. 10 shows the overall changes in the sensing network (consisting of five sensors) for a 2mm cracked sample when compared to its healthy state. The remaining plots in Fig. 10 show the individual contribution of each sensor to this overall change. This overall global response (time history) shows that the all sensors are more sensitive in the region of 0.2 – 0.3 millisecond. This region belongs to the coda part of the signal and has more information.

\* <http://www.isle.org/~sbay/software/orca/>

From earlier study by several researchers, it has been found that coda part of the signals usually have more information on damage state of the structure. This fact is apparent from our present study. Sensor 4 shows an early sensitivity which is expected since the crack runs in between the actuator and the sensor 4. Due to the presence of the crack, the wave front traveling towards sensor 4 gets reflected from the crack flank whereas they reach directly without any reflection for a healthy case and hence an early change is seen. The magnitude of this change increases with increase in the crack length which can be observed in Fig. 12. However over the time period sensor 1 is more sensitive to different crack lengths. The accumulative sensitivity over the time period for each sensor is presented in Table 5.

## 5. CONCLUDING REMARKS

In this paper a guided wave based approach has been used to study wave propagation in complex joint. The sensor signals simulated using this approach for piezoelectric transducers distributed on the surface of the lug joint exhibited a fairly good correlation with the experimental results. The study of the interaction of flexural modes generated by the actuator with the damaged structure was studied. Sensor sensitivity studies offered useful information about the performance of each sensor over time in the presence of a crack induced damage. Results indicated a good correlation for sensor 1 signal, obtained experimentally and through simulations, for a healthy case. The frequency transform of the sensor data was used to characterize damage. It was observed that there was a significant change in the amplitudes associated with 138 KHz frequency for sensors 1 and 2 and 118 KHz frequency for sensor 4. Also, the overall response of sensor signals for both a 2mm crack and 4mm crack was obtained using a distance-based outlier determination technique. The coda part of the signal was found to have significant information on the damage states of the structure. It has been found that the performance of sensor 1 was better than the other sensors for both a 2mm and 4mm crack. Significant reduction of time can be achieved by eliminating redundant sensors, thereby providing information from only the most sensitive sensors. Hence, the sensor sensitivity analysis has a potential application in reducing the computational cost for any defect localization technique.

## ACKNOWLEDGEMENT

This research was supported by the MURI Program, Air Force Office of Scientific Research, grant number: FA9550-06-1-0309; Technical Monitor, Dr. Victor Giurgiutiu.

## REFERENCES

- [1] Dalton, R.P., Cawley, P. and Lowe, M. J. S., "The Potential of Guided Waves for Monitoring Large Areas of Metallic Aircraft Fuselage Structure," *Journal of Nondestructive Evaluation*, **20**(1), 29-46, 2001.
- [2] Victorov, I. A., *Rayleigh and Lamb Waves*, Plenum Press, New York, 1967.
- [3] Rose, J. L., *Ultrasonic Waves in Solid Media*, University Press, Cambridge, 1999.
- [4] Dimitriadis, E. K., Fuller, C. R. and Rogers, C. A., "Piezoelectric Actuators for Distributed Vibration Excitation of Thin Plates," *Journal of Vibration and Acoustics*, **113**, 100-107, 1991.
- [5] Giurgiutiu, V. and Zagari, A. N., "Characterization of Piezoelectric Wafer Active Sensors," *Journal of Intelligent Material Systems and Structures*, **11**(12), 959-976, 2000.
- [6] Kessler, S. S., Spearing, S. M., Atalla, M. J., Cesnik, C. E. S. and Soutis, C., "Damage Detection in Composite Materials using Frequency Response Methods," *Composites: Part B*, **33**, 87-95, 2002.
- [7] Kessler, S. S., Spearing, S. M. and Soutis, C., "Damage Detection in Composite Materials using Lamb Wave Methods," *Smart Materials and Structures*, **11**(2), 269-278, 2002.
- [8] Giurgiutiu, V., "Lamb Wave Generation with Piezoelectric Wafer Active Sensor for Structural Health Monitoring," *Smart Structures and Materials: Smart Structures and Integrated Systems*, 111, 2003.
- [9] Giurgiutiu, V., Bao, J. and Zhao, W., "Piezoelectric Wafer Active Sensor Embedded Ultrasonics in Beams and Plates", *Experimental Mechanics*, **43**(4), 428-449, 2003.
- [10] Giurgiutiu, V., Zagari, A. N., Bao, J., Redmond, J., Roach, D. and Rackow, K., "Active Sensors for Health Monitoring of Aging Aerospace Structures," *International Journal of the Condition Monitoring and Diagnostic Engineering Management*, **5**(3), 2002.

- [11] Ihn, J. B. and Chang F.K., "Pitch-catch Active Sensing Methods in Structural Health Monitoring for Aircraft Structures", *Structural Health Monitoring*, 7(1), 5-19, 2008.
- [12] Bay, S. D. and Schwabacher, M., "Mining Distance-Based Outliers in Near Linear Time with Randomization and a Simple Pruning Rule," *SIGKDD*, Washington, DC, 2003.
- [13] Soni, S., Wei, J., Chattopadhyay, A. and Peralta, P., "Multi-scale Modeling and Experimental Validation for Component Fatigue Life Prediction," *Proceedings of ASME IMECE*, 2007.
- [14] *Abaqus Version 6.7, Abaqus/CAE and Abaqus/Standard*, Simulia World Headquarters, Providence, 2007.
- [15] Barnett, V. and Lewis, T., *Outliers in Statistical Data*, John Wiley & Sons, Chichester, 1994.
- [16] Hawkins, D., *Identification of Outliers*, Chapman and Hall, London, 1980.
- [17] Eskin, E., Arnold, A., Prerau, M., Portnoy, M. and Stolfo, S., "A Geometric Framework for Unsupervised Anomaly Detection: Detecting Intrusions in Unlabeled Data," *Data Mining for Sensitivity Applications*, 2002.
- [18] Knorr, E. M., Ng, R. T. and Tucakov, V., "Distance-based Outliers: Algorithms and Applications," *Vldb Journal: Very Large Databases*, 8(3-4), 237-253, 2000.
- [19] Ramaswamy, S., Rastogi, R. and Shim, K., "Efficient Algorithms for Mining Outliers from Large Data Sets," *Proceedings of the ACM SIGMOD Conference*, 427-438, 2000.